Inorganic Chemistry

Article

pubs.acs.org/IC

Basis for Sensitive and Selective Time-Delayed Luminescence Detection of Hydroxyl Radical by Lanthanide Complexes

Katie L. Peterson, Maximilian J. Margherio, Phi Doan, Kyle T. Wilke, and Valérie C. Pierre*

Department of Chemistry, University of Minnesota, Minneapolis, Minnesota 55455, United States

Supporting Information

ABSTRACT: Molecular probes for the detection of hydroxyl radical (HO•) by time-delayed luminescence spectroscopy directly in water at neutral pH with high sensitivity and selectivity are presented. The bimolecular probes consist of a lanthanide complex with open coordination sites and a reactive pre-antenna composed of an aromatic acid or amide; the latter binds to and sensitizes terbium emission upon hydroxylation by HO•. These probes exhibit long luminescence lifetimes compatible with time-delayed measurements that remove interfering background fluorescence from the sample. Six different reactive pre-antenna (benzoate, benzamide, isophthalate, isophthalamide, trimesate, and trimesamide) and two different terbium complexes [Tb-(1,4,7,10-tetraazacyclododecane-1,4,7-tris(acetic acid)) (Tb-DO3A) and Tb-(1,4,7,10-tetraazacyclododecane-1,7-bis(acetic acid)) (Tb-DO2A)] were evaluated. Of these the trimesamide/Tb-DO3A system enables the most sensitive detection of HO• with an about 1000-fold increase in metal-centered time-delayed emission upon hydroxylation of the pre-antenna to 2-hydroxytrimesamide. Excellent selectivity for both the trimesamide/Tb-DO3A and trimesate/Tb-DO3A systems over other reactive oxygen and nitrogen species are observed. Notably, the increase in metal-centered luminescence intensity is not associated with a decrease in the hydration number (q) of Tb-DO3A, suggesting that the antenna is interacting with the lanthanide via a second sphere coordination environment or that coordination by the antenna occurs by displacement of one or more of the carboxylate arms of DO3A. Formation of a weak ternary complex Tb-DO3A•hydroxytrimesamide was confirmed by temperature-dependent titration and a decrease in K_{app} with increasing temperature.

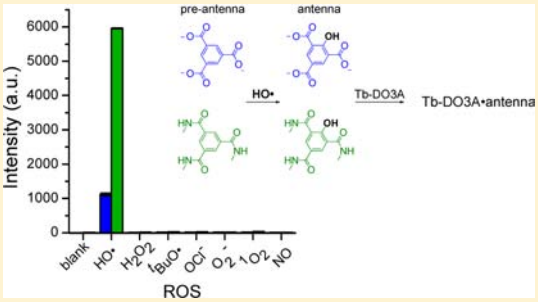

INTRODUCTION

Hydroxyl radical, HO•, with a lifetime in the nanosecond range[1] is the most reactive member of the family of Reactive Oxygen Species (ROS). Production of HO• in vivo is a normal consequence of O_2 oxidation to superoxide (O_2^-) during mitochondrial respiration and enzymes involved in the immune response, primarily NADPH oxidase and xanthine oxidase.[1b,2] Superoxide dismutase catalyzes the conversion of O_2^- to H_2O_2, which can then interact with reduced metals, most commonly Fe(II) or Cu(I), to produce HO•.[2,3] The redox properties of HO•, including a high reduction potential (2.31 V) and interactions with reduced metals, link it to disorders involving the accumulation or miscompartmentalization of redox-active metals, including Alzheimer's, Parkinson's, and Wilson's diseases, and the treatment of β-thalassemia and sickle-cell anemia by red blood cell transfusion.[4] Additionally, the production of HO• above normally regulated levels and the resulting oxidative stress has been implicated in a variety of pathological conditions such as inflammation,[5] reperfusion injury,[6] cancer,[7] as well as aging.[8] The exact role of HO• in many of these physiological processes is not well understood, highlighting the need for an accurate detection method applicable to cellular and tissue imaging to advance biomedical research.

In vitro detection by destructive methods such as electron spin resonance[9] and high pressure chromatography[10] have been reported that exploit the unique reactivity of HO• to generate measurable responses. These methods are, unfortunately, not amenable to continuous monitoring of the ROS. Other fluorescence-based probes have been applied to HO• imaging in cells, but are limited by their sensitivity,[11] selectivity over other ROS (hydrogen peroxide, superoxide, hypochlorite, or alkoxyl radicals),[12] and/or indirect detection systems that do not monitor HO• but instead the products of the reaction of HO• with dimethyl sulfoxide (DMSO).[13] Given the unmet need to detect HO• in biological systems, we recently reported a luminescent lanthanide-based probe for the sensitive and selective detection of HO• in water.[14]

An effective strategy for the detection of HO• via a lanthanide complex involves modulating the ability of an antenna to sensitize the lanthanide luminescence. Altering the efficiency of resonance energy transfer of an antenna to an emissive lanthanide can in turn be achieved by changing either the excited triplet state energy level of the antenna, and/or the antenna-lanthanide distance.[15] Our first generation probe was designed to make use of both of these parameters. This probe

Received: April 17, 2013
Published: July 26, 2013

dx.doi.org/10.1021/ic4009569 | Inorg. Chem. 2013, 52, 9390−9398

consists of a (Tb-DO3A complex and 10 equiv of trimesate (Figure 1). In the absence of HO•, the trimesate does not coordinate, and therefore does not sensitize the emission of the lanthanide ion. Our initial understanding was that the hydroxylated antenna, formed by the reaction of the pre-antenna with HO•, would coordinate to the terbium and displace two water molecules. The coordinated antenna, with a triplet excited state energy level more amenable to terbium emission causes an 11-fold increase in the time-delayed luminescence intensity upon reaction with a steady-state concentration of 0.75 fM HO• over a time of 1 h.[14] Such lanthanide-based detection methods provide several advantages over other optical detection platforms including large Stokes shifts (ca. 200 nm) that eliminate self-absorption issues and enable accurate analyte quantification, and long luminescence lifetimes (ms) that permit time-delayed measurements which remove the interference of background fluorescence.[15] As such, luminescent lanthanide-based detection is increasingly used in probes designed for biomedical research.[14,16] Herein, we investigate the mechanism of the turn-on luminescence of our lanthanide probe for HO•, which further enabled us to design a new system with improved sensitivity and selectivity. The nature and coordinating ability of the antenna was investigated via luminescence lifetime measurements and temperature dependent titrations. The sensitivity of the antennas with the highest turn-on potentials was determined by monitoring HO• produced by the photolysis of H_2O_2. We also demonstrate the ability of the trimesate and trimesamide antennas to selectively respond to HO• over other ROS and reactive nitrogen species (RNS).

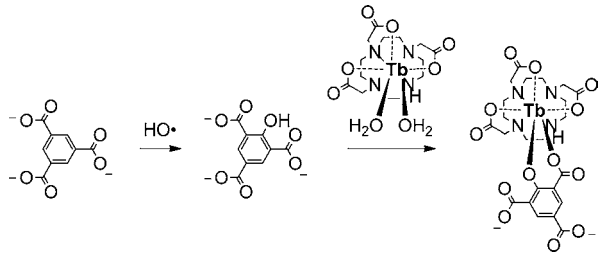

Figure 1. Hydroxyl radical sensing via reaction with trimesate and interaction with Tb-DO3A.

MATERIALS AND METHODS

General Considerations. Chemicals were obtained from commercial suppliers and used without further purification, unless otherwise indicated. All solutions were prepared with deionized water further purified by a Millipore Simplicity UV System (18 MΩ). Experiments were conducted in air at ambient temperature, unless otherwise noted. pH measurements were taken using a Thermo Orion 3 Benchtop pH meter. Fluorescence and phosphorescent measurements were acquired on a Varian Cary Eclipse Fluorescence Spectrophotometer using a quartz cell with a path length of 1 cm, excitation and emission slit widths of 10 nm. Solutions were not degassed prior to measurement of their luminescence spectra and lifetimes.

The following pre-antennas and antennas are commercially available (Sigma-Aldrich) and were used without further purification: **1a**, **1b**, **2a**, **3a**, **4a**, and **4b**. The remaining pre-antennas and antennas, **2b**, **3b**, **5a**, **5b**, **6a**, and **6b** were synthesized according to published literature procedures.[13c,17] Successful synthesis was established by ^{1}H NMR and ESI-MS. Tb-DO3A (1,4,7,10-tetraazacyclododecane-1,4,7-tris(acetic acid)) and Tb-DO2A (1,4,7,10-tetraazacyclododecane-1,7-bis(acetic acid)) were synthesized according to literature precedent for lanthanide carboxylate complexes.[17b,18] The *tert*-butyl protected DO3A and DO2A are commercially available (Macrocyclics).

Time-Delayed Luminescence Intensity of Tb-DO3A with (pre)Antennas (1a−6b). An aqueous solution of (pre)antenna (**1a−6b**) (400 μM) and Tb-DO3A (10.0 μM) in Tris buffer (10 mM, pH 7.2) was titrated into an aqueous solution of Tb-DO3A (10.0 μM) in Tris buffer (10 mM, pH 7.2). The time-delayed emission profile was recorded in the presence of 0−200 μM of (pre)antenna (**1a−6b**). Measurements were recorded with a time delay of 0.1 ms, excitation and emission slit widths of 10 nm, and at a temperature of 20 °C. The following excitation wavelengths were used: **1a**/**b**, λ_{ex} = 321 nm; **2a**/**b**, λ_{ex} = 333 nm; **3a**/**b**, λ_{ex} = 333 nm; **4a**/**b**, λ_{ex} = 324 nm; **5a**/**b**, λ_{ex} = 331 nm; **6a**/**b**, λ_{ex} = 328 nm. The luminescence response was reported as the integrated emission intensity from 470−635 nm. The experiment was repeated in triplicate (n = 3).

Luminescence Lifetimes and Hydration Number (q). The luminescence decay of an aqueous solution of hydroxylated antenna, **1a−6b**, (500 μM), Tb-DO3A or Tb-DO3A (50 μM), and Tris (10 mM for Tb-DO3A and 100 mM for Tb-DO2A, pH 7.2) was measured. For measurements in D_2O, the samples were lyophilized and redissolved in D_2O three times prior to analysis. All decay measurements monitored the emission at 545 nm, using an initial time delay of 0.01 ms, delay increments of 0.1 or 0.2 ms, total decay time of 10 ms, and excitation and emission slit widths of 10 nm at a temperature of 20 °C. Luminescence lifetimes (τ) were determined by fitting the data to an exponential decay. The hydration number was calculated according to the following equation developed by Horrocks:[19] $q = 4.2[(1/\tau_{H2O}) - (1/\tau_{D2O})]$. Data was collected in triplicate (n = 3).

Effect of Temperature on Formation of the Tb-DO3A·Hydroxytrimesamide Ternary Complex. An aqueous solution of antenna (**6b**) (100 μM) and Tb-DO3A (10.0 μM) in Tris buffer (10 mM, pH 7.2) was titrated into an aqueous solution of Tb-DO3A (10.0 μM) in Tris buffer (10 mM, pH 7.2). The time-delayed emission profile was recorded in the presence of 0−10 μM of antenna (**6b**). Measurements were recorded with a time delay of 0.1 ms, excitation wavelength of 328 nm, excitation and emission slit widths of 10 nm, and at temperatures of 10, 20, 40, 60, and 80 °C. The luminescence response was reported as the integrated emission intensity from 470−635 nm. At each temperature, the experiment was repeated in triplicate (n = 3).

Monitoring HO• Produced by Photolysis of H_2O_2. An aqueous solution of H_2O_2 (50 μM) and pre-antenna (**2a**, **3a**, **5a**, or **6a**) (103 μM) were added to a quartz cuvette. The solution (3 × 4 mL total volume) was then irradiated in the quartz cell for 1 h at 254 nm with a Spectroline hand-held UV lamp. An aliquot (1.00 mL) was removed from the irradiated cell at 0, 5, 10, 15, 20, 25, 30, 45, and 60 min. Tris buffer (12 mM, pH 7.2), and Tb-DO3A (12 μM) were added to the aliquot. The luminescence intensity was measured with a time delay of 0.1 ms, excitation and emission slit widths of 10 nm, and at a temperature of 20 °C. The following excitation wavelengths were used for luminescence measurements: **2a**, λ_{ex} = 333 nm; **3a**, λ_{ex} = 333 nm; **5a**, λ_{ex} = 331 nm; **6a**, λ_{ex} = 328 nm. The luminescence response is reported as the integrated emission intensity from 470−635 nm. The experiment was repeated in triplicate (n = 3).

Selectivity versus ROS and RNS. ROS and RNS were administered to aqueous solutions of the pre-antennas (**3a** or **6a**) as described below. After stirring the reaction mixtures at room temperature for 30 min, Tris buffer, and Tb-DO3A were added to a 1000 μL aliquot of the reaction mixture resulting in the following final concentrations: Tris buffer (12 mM, pH = 7.2), Tb-DO3A (12 μM), pre-antenna (**3a** or **6a**) (97 μM). The luminescence intensity was measured with a time delay of 0.1 ms, excitation and emission slit widths of 10 nm, and at a temperature of 20 °C. The following excitation wavelengths were used for luminescence measurements: **3a**, λ_{ex} = 333 nm; **6a**, λ_{ex} = 328 nm. The luminescence response was reported as the integrated emission intensity from 470−635 nm. Each experiment was repeated in triplicate (n = 3).

dx.doi.org/10.1021/ic4009569 | *Inorg. Chem.* 2013, 52, 9390−9398

Hydroxyl Radical (HO•). An aqueous solution of H_2O_2 (50 μM) and pre-antenna (**3a** or **6a**) (103 μM) was irradiated in a quartz cuvette for 30 min at 254 nm using a Spectroline hand-held UV lamp.

Hydrogen Peroxide (H_2O_2). An aqueous solution of H_2O_2 (16.4 mM) and pre-antenna (**3a** or **6a**) (103 μM) was stirred for 30 min at room temperature.

tert-Butoxy Radical (^{t}BuO•). ^{t}BuO• was generated in situ according to the procedure of Winston et al.[20] Briefly, an aqueous solution of *tert*-butyl hydrogen peroxide (2.0 μM), $[Fe(bpy)_3(ClO_4)_2]$ = 0.52 μM and pre-antenna (**3a** or **6a**) (103 μM) was stirred for 30 min at room temperature ***Caution!*** *The iron perchlorate salt is potentially explosive and should be handled with care.*

Hypochlorite (OCl^-). An aqueous solution of hypochlorite (103 μM) and pre-antenna (**3a** or **6a**) (103 μM) was stirred for 30 min at room temperature.

Superoxide (O_2^-). Solid KO_2 (1.1 mg, 0.015 mmol, 3.9 mM final concentration) was added to an aqueous solution of pre-antenna (**3a** or **6a**) (103 μM), and the reaction mixture was stirred for 30 min at room temperature. Note that the solid KO_2 was added directly to the solution of pre-antenna and not administered from a stock solution since the lifetime of O_2^- is insufficient to make stock solutions.

Singlet Oxygen ($^1O_2$). An aqueous solution of Rose Bengal (0.52 μM) and pre-antenna (**3a** or **6a**) (103 μM) was purged three times with O_2 and stirred under irradiation with UV light using a 90 W Halogen Flood lamp for 30 min.

Nitric Oxide (NO). An aqueous solution of spermine NONOate (520 μM final concentration, delivered from a stock solution in 0.01 M NaOH) and pre-antenna (**3a** or **6a**) (103 μM) was adjusted to pH 5 with HCl and stirred for 30 min at room temperature. The reaction mixture was readjusted to pH 7.0 with NaOH prior to analysis.

RESULTS AND DISCUSSION

Effect of the Antenna. The probe consists of two parts: a lanthanide complex with at least two open coordination sites initially occupied by solvent molecules and a pre-antenna that coordinates to and sensitizes terbium only after reaction with HO•. Our first step in optimizing its design so as to achieve maximum sensitivity for HO• detection focuses on the nature of the pre-antenna. Six different pre-antenna/antenna pairs were investigated: salicylicate, salicylamide, isophthalate, isopthalamide, trimesate, and trimesamide (Figure 2). The acids were selected because of their previous incorporation into HO• detection systems,[10d,11b,c,14,21] while the amides were chosen because of reports by Raymond and co-workers that demonstrated that the isophthalamide and trimesamide based ligands are efficient sensitizers of lanthanide (Sm, Eu, Tb, Dy, Ho) emission.[22] The trimesate and trimesamide antennas have the additional benefit of three equivalent primary reaction sites for HO•; reaction at either site results in the same product. Thus, the investigated antennas were selected to maximize both HO• response and relative time-delayed luminescence intensity.

The probe further relies on a substantial difference in sensitizing ability between the antenna and the pre-antenna. In each case, the time-delayed excitation, time-delayed emission, and fluorescence intensity of Tb-DO3A is substantially higher for the hydroxylated antenna than for its corresponding nonhydroxylated analog (Supporting Information, Figure S1). For example, trimesamide (**6a**) does not sensitize Tb effectively, but upon reaction with HO• it yields the powerful hydroxytrimesamide (**6b**) antenna (Figure 3). To evaluate which pre-antenna/antenna pair yielded the highest response, we began our investigation by determining the ability of each aromatic compound to sensitize terbium emission under identical conditions. Note that each pre-antenna/antenna pair requires a different excitation wavelength to maximize the

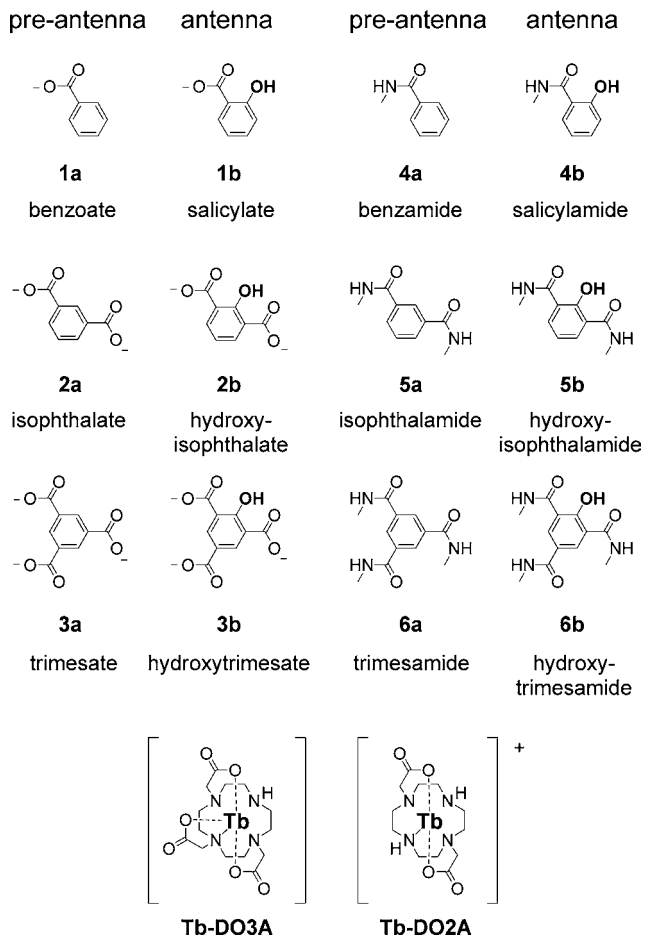

Figure 2. Chemical structures of pre-antennas, antennas, Tb-DO3A, and Tb-DO2A.

luminescence intensity in the presence of the hydroxylated antenna. In each case, this wavelength was selected from the time-delayed excitation profiles of the hydroxylated antenna/Tb-DO3A mixture (Supporting Information, Figures S2–S7). Keeping all other experimental conditions constant, the ability of each hydroxylated antenna to modulate Tb-DO3A luminescence can be directly compared (Figure 4). Alternatively, this turn-on ability can also be expressed by the change in relative integrated emission intensity ($\Delta(I/I_0) = I/I_{0\ Tb\bullet antenna} - I/I_{0\ Tb\bullet pre\text{-}antenna}$) as calculated with 10 equiv of the antenna per Tb-DO3A (Table 1). Note that these comparisons are possible because the same excitation wavelength and photomultiplier tube (PMT) voltage was used for the pre-antenna and antenna in each pair; all other experimental parameters were kept constant for all pre-antenna/antenna pairs. The high $\Delta I/I_0$ values, about 1000-fold increase for pre-antenna/antenna pairs **2**, **3**, **5**, and **6** indicate that the hydroxyisophthalate (**2b**), hydroxytrimesate (**3b**), hydroxyisophthalamide (**5b**), and hydroxytrimesamide (**6b**) antennas are significantly more efficient antennas for Tb-DO3A than the salicylate (**1b**) and salicylamide (**4b**).

In addition to a high luminescence intensity, the ideal antenna for HO• detection is able to respond to the analyte when it is present in low concentrations (Figure 5). With concentrations in the micromolar range, the hydroxytrimesate (**3b**) and hydroxytrimesamide (**6b**) cause the largest increases in the luminescence of Tb-DO3A (Figure 6). The 500-fold luminescence increase of **3b** and **6b** when present at 0.5 equiv

dx.doi.org/10.1021/ic4009569 | *Inorg. Chem.* 2013, 52, 9390–9398

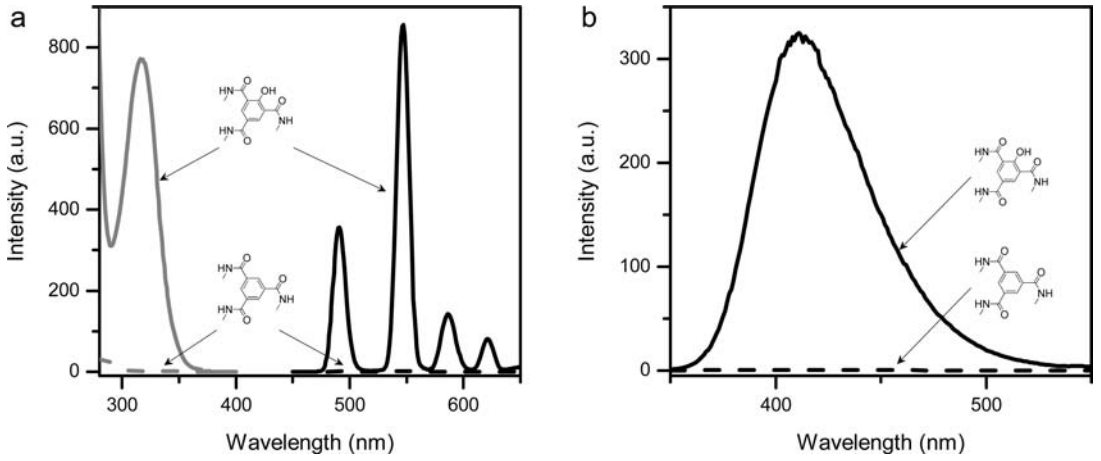

Figure 3. (a) Time-delayed excitation (gray), time-delayed emission (black), and (b) fluorescence profiles of Tb-DO3A in the presence of pre-antenna **6a** (dashed) or hydroxylated antenna **6b** (solid). Conditions: [Tb-DO3A] = 10 μM, [(pre)antenna, **6a** or **6b**] = 100 μM, [Tris] = 10 mM, pH 7.2, slit widths (excitation and emission) = 10 nm, T = 20 °C. Phosphorescence parameters for (a): λ_{em} = 545 nm, λ_{ex} = 328 nm, time delay = 0.1 ms. Fluorescence parameters for (b): λ_{ex} = 314 nm.

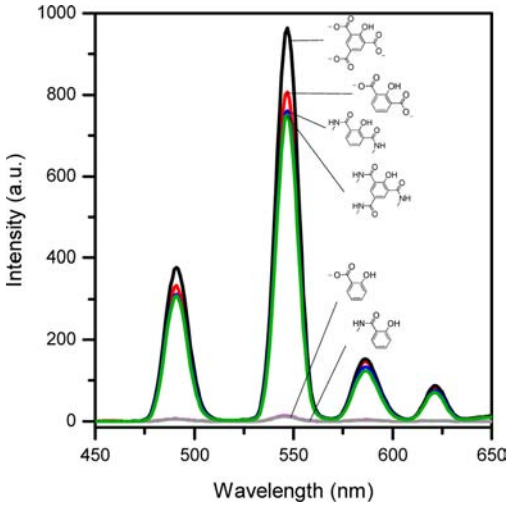

Figure 4. Time-delayed emission of Tb-DO3A in the presence of hydroxylated antennas: **1b** (magenta), **2b** (red), **3b** (black), **4b** (gray), **5b** (blue), and **6b** (green). Conditions; [Tb-DO3A] = 10 μM, [antenna] = 100 μM, [Tris] = 10 mM, pH 7.2, time delay = 0.1 ms, slit widths (excitation and emission) = 10 nm, T = 20 °C. Excitation wavelengths (λ_{ex}): **1b**, 321 nm; **2b**, 333 nm; **3b**, 333 nm; **4b**, 324 nm; **5b**, 331 nm; **6b**, 328 nm.

to Tb-DO3A, make these antennas the most promising candidates for the detection of HO• at biologically relevant concentrations. Interestingly, for some systems (hydroxyisophthalate, **2b**, hydroxytrimesate, **3b**, hydroxyisophthalamide, **5b**, hydroxytrimesamide, **6b**), the maximum excitation wavelength is red-shifted at higher concentration of antenna (Supporting Information, Figures S2–S7). These observations suggest that at higher concentrations, the antenna is not fully solvated but is likely aggregated, resulting in multiple different luminescing states.

Coordinating Ability of the Antenna and Formation of a Ternary Complex. The substantial increase in time-delayed luminescence of the terbium center up to 700-fold for a 1:1 mixture of 2-hydroxytimesamide and Tb-DO3A in the μM range strongly implies a simple equilibrium and the formation of ternary complex between the hydroxylated antenna and the lanthanide complex. These results are consistent with prior observations by Gunnlaugsson and co-workers with similar systems.[16b,21] With this in mind, our initial hypothesis was that the substantial increase in metal-centered emission was due to direct coordination of the hydroxylated antenna to the terbium ion. One should note, however, that the data do not necessarily prove that the antenna is directly coordinated to the metal.

To establish the presence of this ternary complex, we evaluated the effect of temperature on the binding curve. Energy transfer from the antenna to the lanthanide can in

Table 1. Relative Integrated Emission Intensity (I/I_0) for Each Pre-Antenna and Antenna Pair Representing the Turn-on Ability of Each Pre-Antenna[a]

pre-antenna				antenna				
		λ_{ex} (nm)	I/I_0			λ_{ex} (nm)	I/I_0	$\Delta I/I_0$
1a	benzoate	321	1.2	**1b**	salicylate	321	23	**22**
2a	isophthalate	333	1.1	**2b**	hydroxyisophthalate	333	1141	**1140**
3a	trimesate	333	1.4	**3b**	hydroxytrimesate	333	1131	**1130**
4a	benzylamide	324	1.8	**4b**	salicylamide	324	25	**23**
5a	isophthalamide	331	1.0	**5a**	hydroxyisophthalamide	331	1104	**1103**
6a	trimesamide	328	3.9	**6a**	hydroxytrimesamide	328	992	**988**

[a]Conditions: [Tb-DO3A] = 10 μM, [(pre)antenna] = 100 μM, [Tris] = 10 mM, pH 7.2, time delay =0.1 ms, slit widths (excitation and emission) = 10 nm, T = 20°C. I = integrated emission intensity from 470–635 nm. $\Delta(I/I_0) = I/I_{0\ Tb\bullet antenna} - I/I_{0\ Tb\bullet pre\text{-}antenna}$. Each value represents the average of 3 replicates (n = 3).

dx.doi.org/10.1021/ic4009569 | Inorg. Chem. 2013, 52, 9390–9398

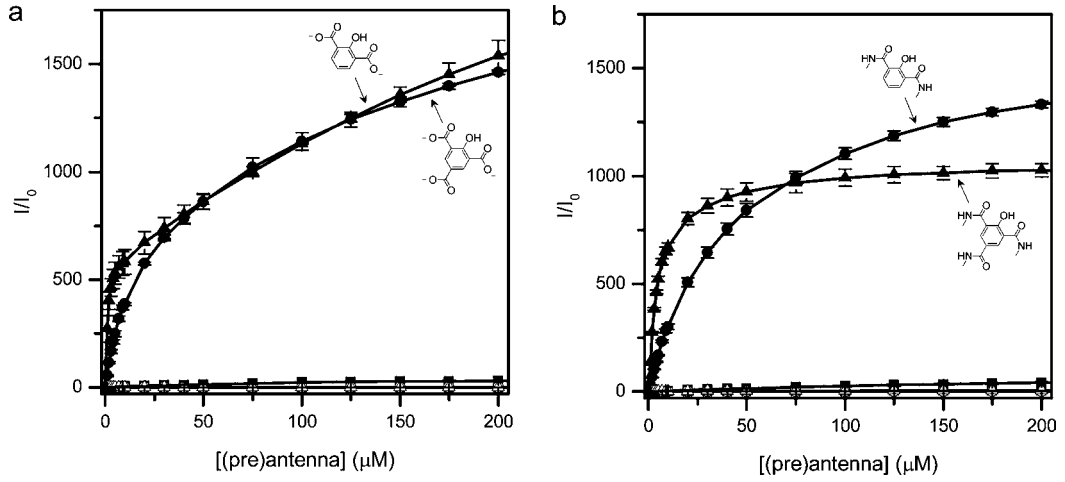

Figure 5. Relative time-delayed luminescence (I/I_0) of Tb-DO3A as a function of increasing concentrations of (a) acid (pre)antenna: **1a** (open square), **1b** (filled square), **2a** (open circle), **2b** (filled circle), **3a** (open triangle), **3b** (filled triangle), and (b) amide (pre)antenna: **4a** (open square), **4b** (filled square), **5a** (open circle), **5b** (filled circle), **6a** (open triangle), **6b** (filled triangle). Conditions: [Tb-DO3A] = 10 μM, [(pre)antenna] = 0–200 μM, [Tris] = 10 mM, pH 7.2, time delay =0.1 ms, slit widths (excitation and emission) = 10 nm, T = 20 °C. Excitation wavelengths: **1a/b**, λ_{ex} = 321 nm; **2a/b**, λ_{ex} = 333 nm; **3a/b**, λ_{ex} = 333 nm; **4a/b**, λ_{ex} = 324 nm; **5a/b**, λ_{ex} = 331 nm; **6a/b**, λ_{ex} = 328 nm. I = integrated emission intensity from 470–635 nm. Results are mean ± SD (n = 3).

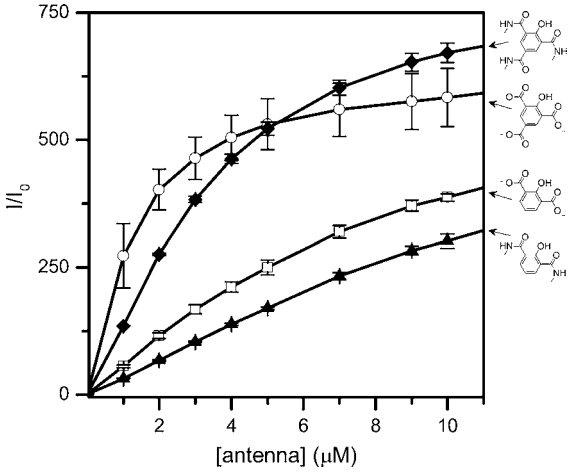

Figure 6. Relative time-delayed luminescence (I/I_0) of Tb-DO3A as a function of increasing concentrations of antenna: **2b** (open square), **3b** (open circle), **5b** (filled triangle), and **6b** (filled diamond). Conditions: [Tb-DO3A] = 10 μM, [antenna] = 0–10 μM, [Tris] = 10 mM, pH 7.2, time delay = 0.1 ms, slit widths (excitation and emission) = 10 nm, T = 20 °C. Excitation wavelengths: **2b**, λ_{ex} = 333 nm; **3b**, λ_{ex} = 333 nm; **5b**, λ_{ex} = 331 nm; **6b**, λ_{ex} = 328 nm. I = integrated emission intensity from 470–635 nm. Results are mean ± SD (n = 3).

theory occur either via a static or a dynamic mechanism. The first involves equilibrium and formation of a ternary complex, Tb-DO3A·antenna, which is entropically disfavored.

$$\text{Tb-DO3A} + \text{antenna} \rightleftharpoons \text{Tb-DO3A·antenna}$$

Assuming that energy transfer from the triplet excited state of the antenna to the ^{5}D state of the lanthanide is relatively constant in the temperature range considered, an increase in the temperature would shift the equilibrium to the left, resulting in a decrease in K_{app}. On the other hand, if no ternary complex is formed, sensitization of the lanthanide ion would occur in a purely dynamic or collisional mechanism that would be favored at high temperature. In this case, K_{app}, would increase as temperature increases. It is apparent from the temperature-dependence titration of Tb-DO3A with 2-hydroxytrimeasemide (**6b**) that K_{app} decreases as the temperature increases from 5 to 80 °C (Figure 7). This decrease confirms the formation of a ternary complex between Tb-DO3A and the hydroxylated antenna which is the basis of the substantial turn-on for our probe.

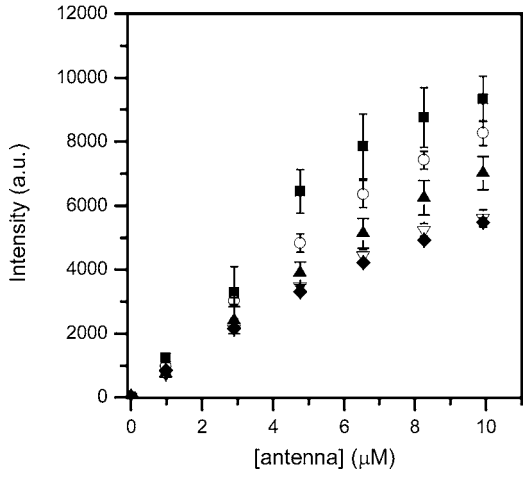

Figure 7. Relative time-delayed luminescence (I/I_0) of Tb-DO3A as a function of increasing concentrations of hydroxytrimesate antenna **6b** at different temperatures: 5 °C (filled square), 20 °C (open circle), 40 °C (filled upright triangle), 60 °C (open downward triangle), and 80 °C (filled diamond). Conditions: [Tb-DO3A] = 10 μM, [antenna] = 0–10 μM, [Tris] = 10 mM, pH 7.2, time delay = 0.1 ms, excitation wavelength = 328 nm, slit widths (excitation and emission) = 10 nm. I = integrated emission intensity from 470–635 nm. Results are mean ± SD (n = 3).

One possibility to evaluate the binding mode of the hydroxylated antenna and the structure of the ternary complex is to determine the number of inner-sphere water molecules directly coordinated on the lanthanide ion. This was achieved by measuring the luminescence lifetimes (τ) for the terbium centered emission in H_2O and D_2O according to the method of

dx.doi.org/10.1021/ic4009569 | Inorg. Chem. 2013, 52, 9390–9398

Table 2. Luminescence Lifetimes and Corresponding Hydration Numbers (q) for Tb-DO3A and Tb-DO2A in the Presence of Hydroxylated Antennas[a]

		Tb-DO3A				Tb-DO2A			
		τ_{H_2O} (ms)	τ_{D_2O} (ms)	q	Δq^b	τ_{H_2O} (ms)	τ_{D_2O} (ms)	q	Δq^c
1b	salicylate	1.04	1.76	**1.6**	**0.4**	1.08	2.38	**2.1**	**0.9**
2b	hydroxyisophthalate	1.14	2.19	**1.8**	**0.2**	1.05	2.33	**2.2**	**0.8**
3b	hydroxytrimesate	0.91	1.82	**2.3**	**−0.3**	1.05	2.24	**2.1**	**0.9**
4b	salicylamide	1.01	1.80	**1.8**	**0.2**	1.08	2.20	**2.0**	**1.0**
5a	hydroxyisophthalamide	0.99	2.22	**2.3**	**−0.3**	1.04	2.40	**2.3**	**0.7**
6a	hydroxytrimesamide	0.86	2.14	**2.9**	**−0.9**	1.02	2.12	**2.1**	**0.9**

[a]Conditions: [Tb-DO3A or Tb-DO3A] = 50 μM and [antenna] = 500 μM, [Tris] = 10 mM for Tb-DO3A and 100 mM for Tb-DO2A, pH 7.2, λ_{em} = 545 nm, time delay = 0.1 ms, slit widths (excitation and emission) = 10 nm, T = 20°C. Each value represents the average of 3 replicates (n = 3). [b]$\Delta q = q_{\text{Tb-DO3A}} - q_{\text{Tb-DO3A•antenna}}$. [c]$\Delta q = q_{\text{Tb-DO2A}} - q_{\text{Tb-DO2A•antenna}}$.

Horrocks.[19] The number of bound water molecules (q) can then be calculated as follows:

$$q = 4.2[(1/\tau_{H_2O}) - (1/\tau_{D_2O})]$$

Of the nine coordination sites available for terbium, the heptadentate ligand DO3A leaves two sites open for water molecule coordination, while the hexadentate DO2A leaves three. Assuming a salicylate binding mode as observed by Raymond et al. in lanthanide hydroxyisophthalamide complexes,[17b] in each case coordination of the hydroxylated antenna on the terbium was expected to reduce the q value by two (Figure 1).

The surprising results of this experiment are given in Table 2. For the parent Tb-DO3A complex, there is no noticeable change of the hydration number regardless of the hydroxylated antenna considered; $\Delta q = q_{\text{Tb-DO3A}} - q_{\text{Tb-DO3A•antenna}} = 0 \pm 0.4$ in the presence of 10 equiv of hydroxylated antenna. These results thus suggest that, in contradiction with our initial theory, none of the efficient antennas (**2b**, **3b**, **5b**, **6b**) replace the two inner-sphere water molecules in Tb-DO3A. One could postulate that this lack of binding is due to steric hindrance around the two open coordination sites on the terbium ion. In the hope of favoring direct coordination of the hydroxylated antenna by replacing the two inner sphere water molecules, which would in turn increase the luminescence of the ternary complex and the sensitivity of the probe, we further investigated the less stable but less sterically hindered Tb-DO2A which contains three open coordination sites. Opening one more coordination site does enable every hydroxylated antenna to coordinate the terbium, $\Delta q = 1 \pm 0.3$, however, in each case, two inner-sphere water molecules still remain. Note that this does not necessarily indicate that the hydroxylated antennas do not coordinate the terbium ion in the case of Tb-DO3A. We cannot distinguish from this experiment alone between complete lack of ligation by the aromatic antenna (in which case the terbium would be solely complexed by the polyaminocarboxylate ligand) and coordination of the antenna in a salicylate (or other) binding mode concomitant with release of two carboxylate arms from the DO3A or DO2A ligand. Both cases results in a lanthanide complex with two inner-sphere water molecules. Also note that the conclusions from our system may not apply to other polyaminorcarboxylate lanthanide complexes. While investigating the ability of salicylate-based antenna to coordinate and sensitize a terbium complex with a tridimethylacetamide cyclen chelate; Gunnlaugsson and co-workers determined that the cationic complex does interact with negatively charged aromatic acid antenna through either a bidentate binding mode utilizing both oxygen of the carboxylic acids, a salicylate binding mode involving both the carboxylate and the phenolate, or in a monodentate version solely via the phenolate.[21,23]

Monitoring Production of HO• by Time-Delayed Luminescence. The purpose of the previous studies was to optimize the two component system for the detection of HO• by time-delayed luminescence with higher sensitivity. The ability of the isophthalate (**2a**), trimesate (**3a**), isophthalamide (**5a**), and trimesamide (**6a**) pre-antennas to detect a low steady-state concentration of HO• in the femtomolar range in the presence of Tb-DO3A is given in Figure 8.[14,24] In each of our studies, HO• was generated by photolysis of H_2O_2 (irradiation λ = 254 nm). The near diffusion limited rate constant of HO• with aromatics systems (10^9 M^{-1} s^{-1})[24] results in the formation of hydroxylated antenna and ternary complex in the μM concentration range. Given the brightness of the ternary complex, and the dullness of the unreacted probe, this causes a substantial increase in luminescent intensity even with reaction times under 1 h. Moreover, the initial linear response to HO• is indicative of the pseudo-zeroth order kinetics of the system, as is expected given the flooding conditions of antenna and the low, steady-state concentration of HO•. After 30 min, the relative time-delayed luminescence intensity increased by 77-fold in the presence of trimesamide (**6a**) and 46-fold with the trimesate (**3a**) pre-antenna. The isophthalate (**2a**) and isophthalamide (**5a**) pre-antennas yielded much lower increase in metal-centered emissions in the presence of HO•, 12-fold for **2a**, and 4-fold **5a**. The increased sensitivity of the trimesate (**3a**) and especially the trimesamide (**6a**) pre-antennas over the isophthalate (**2a**) and isophthalamide (**5a**) are partly attributed to the symmetry of the **3a** and **6a**. For these pre-antennas, only one product can be formed upon reaction with HO•. Hydroxylation of isophthalate and isophthalamide, on the other hand, can occur at three different ring positions, only two of which favor lanthanide coordination and sensitization. Moreover, the luminescence increase with the trimesamide system (**6a**) is significantly greater than with the trimesate (**3a**). The 77-fold increase in terbium luminescence with the use of trimesamide illustrate a distinct advantage of our second generation probe over our initial trimesate and Tb-DO3A detection system.[14] Importantly, the trimesamide (**6a**)/Tb-DO3A system is able to respond to HO• produced from the photolysis of biologically relevant concentrations of H_2O_2, as the biological concentration of H_2O_2 during periods of oxidative stress in an inflammatory environment can reach about 100 μM.[2,25]

dx.doi.org/10.1021/ic4009569 | Inorg. Chem. 2013, 52, 9390−9398

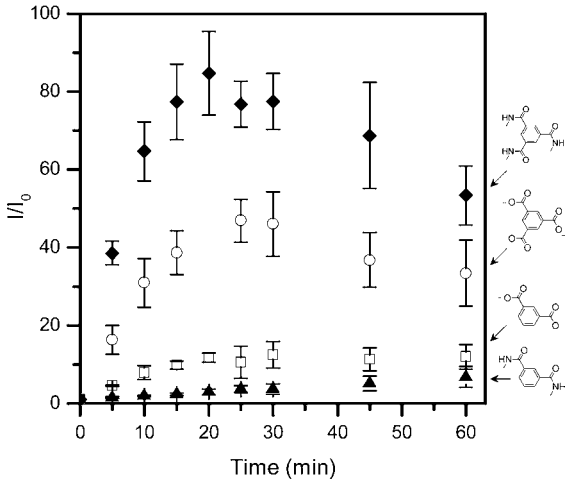

Figure 8. Relative time-delayed luminescence response (I/I_0) of Tb-DO3A in the presence of pre-antenna **2a** (open square), **3a** (open circle), **5a** (filled triangle), and **6a** (filled diamond) to HO• generated by photolysis of H_2O_2. Experimental conditions: [pre-antenna] = 103 μM, [H_2O_2] = 50 μM, photolysis wavelength = 254 nm. Phosphorescence conditions: [Tb-DO3A] = 12 μM, [pre-antenna] = 97 μM, [Tris] = 12 mM, pH 7.2, time delay = 0.1 ms, slit widths (excitation and emission) = 10 nm, T = 20 °C. Excitation wavelengths: **2a**, λ_{ex} = 333 nm; **3a**, λ_{ex} = 333 nm; **5a**, λ_{ex} = 331 nm; **6a**, λ_{ex} = 328 nm. I = integrated emission intensity from 470−635 nm. Results are mean ± SD (n = 3).

In comparison, the earlier detection system based on the fluorescence of hydroxylated terephthalate has an estimated detection limit of 50 nM,[11c] although more recent systems can monitor HO• in the fM range.[26] A probe designed by Sho and co-workers has the advantage of monitoring HO• generated by Fenton chemistry with mM concentrations of H_2O_2 ratiometrically although it is characterized by a limited turn-on of less than 4-fold.[11f] Unfortunately, comparison of the sensitivity of our probe with other fluorescence-based HO• detection methods is problematic given the varying procedures used for the generation of HO•, such as Fenton chemistry or photolysis of H_2O_2 or $NaNO_3$. Moreover, the concentrations of the reagents or irradiation source power impact the amount of HO• produced, and the concentrations of HO• are seldom measured or reported. Keeping this in mind, the sensitivity of the TbDO3A/trimesamide system remains comparable to or better than other luminescent probes reported.

Selectivity for HO• over Other ROS and RNS. Given the very low concentration of HO• in biological and environmental systems compared to other ROS and RNS, the selectivity of the probe versus these other reactive species is as crucial as the sensitivity of the probe. The ability of the trimesate (**3a**) and trimesamide (**6a**) pre-antennas to selectively respond to HO• over other ROS is given in Figure 9. In both cases, excellent selectivity was observed; a greater than 180-fold or 75-fold selectivity for HO• over other ROS was observed for the trimesamide (**6a**) and trimesate (**3a**) pre-antennas, respectively, although substantially higher concentrations of the competing ROS/RNS were used. Importantly, the response of our probes to H_2O_2 and NO that are present at orders of magnitude higher concentrations and have longer life times in vivo is negligible.[1] This excellent selectivity was anticipated given our detection system. Hydroxylation of the antenna is key not only to binding the aromatic acid to the lanthanide complex but also to adjusting the energy level of its triplet excited state so as to allow maximum energy transfer to the lanthanide ion. Since this hydroxylation is not possible with other ROS and RNS, these other species were postulated not to turn on the luminescence of our probe, hence the observed selectivity.

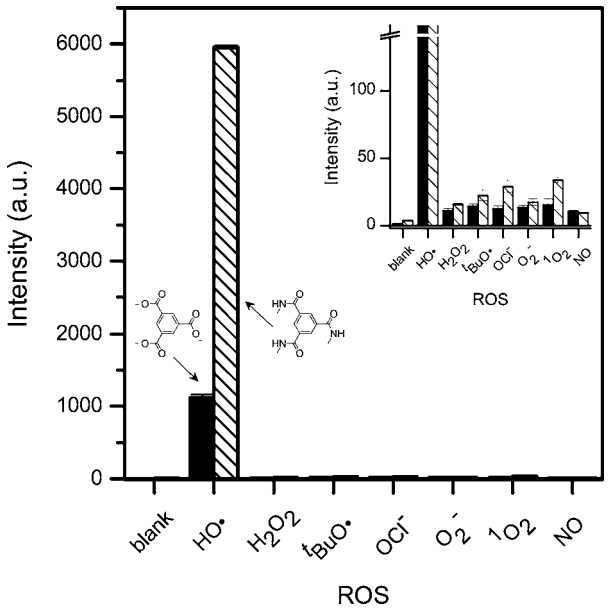

Figure 9. Selectivity of Tb-DO3A and **3a** (filled bars) or **6a** (striped bars) for HO• versus other ROS. Experimental conditions: [**3a** or **6a**] = 103 μM, [HO•] = fM range, [H_2O_2] = 16.4 mM, [^{t}BuO•] = 2.0 μM, [OCl$^-$] = 103 μM, [$O_2^{\bullet-}$] = 3.9 mM, [$^1O_2$] = μM range, [NO] = 1.0 mM, reaction time = 30 min, photolysis wavelength = 254 nm, room temperature. Phosphorescence conditions: [Tb-DO3A] = 12 μM, [pre-antenna] = 97 μM, [Tris] = 12 mM, pH 7.2, time delay = 0.1 ms, slit widths (excitation and emission) = 10 nm, T = 20 °C. Excitation wavelengths: **3a**, λ_{ex} = 333 nm; **6a**, λ_{ex} = 328 nm. Blank = 100 μM **3a** or **6a**, 10 μM Tb-DO3A, 10 mM Tris buffer. I = integrated emission intensity from 470−635 nm. Results are mean ± SD (n = 3).

Comparison with other reported systems is limited since the selectivity of most probes for HO• over other ROS and RNS is seldom reported. Moreover, in most selectivity studies published, the concentration of HO• is typically irrelevant to biological or environmental conditions. In some of the most studied systems, selectivity for HO• toward other highly reactive species such as $O_2^{\bullet-}$, OCl$^-$, ^{t}BuO• limits the utility of the systems.[12] Since they respond to multiple oxidative species, these detection systems serve as general indicators of oxidative stress and not as probes for hydroxyl radical.[12b,c] Aside from our probe, the nitroxide radical based detection systems demonstrate the highest selectivity for HO•, but are unfortunately limited in that they detect not hydroxyl radical itself, but the products of the reaction of HO• with DMSO.[13a] In comparison, the metal-centered luminescence intensity of the trimesamide (**6a**)/Tb-DO3A system showed excellent selectivity for a steady state concentration of HO• in the fM range, compared H_2O_2, $O_2^{\bullet-}$, and NO in the mM range.

■ CONCLUSIONS

Molecular probes for the time-delayed luminescence detection of HO• are reported. The bimolecular probes consist of an aromatic acid that reacts with HO• to produce hydroxylated chromophores that readily bind to Tb-DO3A and sensitize lanthanide-centered emission. Of the six antenna investigated

dx.doi.org/10.1021/ic4009569 | Inorg. Chem. 2013, 52, 9390−9398

(benzoate, benzamide, isophthalate, isophthalamide, trimesate, and trimesamide), the trimesamide (**6a**) demonstrates the highest sensitivity with 77-fold increase in time-delayed luminescence upon reaction with steady state fM concentration of HO• after 30 min. In addition, the system displays excellent selectivity, greater than 180-fold, over other ROS and RNS species. Surprisingly, the increase in luminesce intensity does not correlate with a decrease in the hydration number (q) of the terbium center for TbDO3A. Nonetheless, temperature-dependent titrations confirmed the formation of a ternary complex, Tb-DO3A•hydroxytrimesamide, in which the antenna binds the terbium either by displacing two carboxylate arms or via a second sphere coordination environment. The turn-on mechanism, selectivity, and sensitivity of this system express significant gains over our first generation sensor based on the reactivity of trimesate and Tb-DO3A time-delayed luminescence.[14]

■ ASSOCIATED CONTENT

Ⓢ Supporting Information

Time-delayed excitation and emission luminescence profiles, and fluorescence emission profiles for Tb-DO3A in the presence of pre-antenna/antenna pairs. Time-delayed excitation and emission luminescence profiles, and fluorescence emission profiles Tb-DO3A upon titration with **1b**−**6b**. This material is available free of charge via the Internet at http://pubs.acs.org.

■ AUTHOR INFORMATION

Corresponding Author

*E-mail: pierre@umn.edu.

Notes

The authors declare no competing financial interest.

■ ACKNOWLEDGMENTS

This work was supported by the National Science Foundation Grant CAREER 1151665. Support to K.L.P. from the NIH-CBITG (GM 08700) and to M.M. through a Heisig Fellowship from the Department of Chemistry of the University of Minnesota are gratefully acknowledged.

■ ABBREVIATIONS

DMSO, dimethyl sulfoxide; DO3A, 1,4,7,10-tetraazacyclododecane-1,4,7-tris(acetic acid); DO2A, 1,4,7,10-tetraazacyclododecane-1,7-bis(acetic acid); ESI-MS, electrospray ionization mass spectrometry; H_2O_2, hydrogen peroxide; HO•, hydroxyl radical; NADPH, nicotinamide adenine dinucleotide phosphate; NMR, nuclear magnetic resonance; NO, nitric oxide; OCl^-, hypochlorite; O_2^-, superoxide; $^1O_2$, singlet oxygen; PMT, photomultiplier tube; RNS, reactive nitrogen species; ROS, reactive oxygen species; ^{t}BuO•, *tert*-butoxy radical; Tb, terbium; Tris, 2-amino-2-hydroxymethyl-propane-1,3-diol

■ REFERENCES

(1) (a) Dickinson, B. C.; Chang, C. J. *Nat. Chem. Biol.* **2011**, *7*, 504−511. (b) Winterbourn, C. C. *Nat. Chem. Biol.* **2008**, *4*, 278−286.
(2) Valko, M.; Leibfritz, D.; Moncol, J.; Cronin, M. T. D.; Mazur, M.; Telser, J. *Int. J. Biochem. Cell Biol.* **2007**, *39*, 44−84.
(3) Prousek, J. *Pure Appl. Chem.* **2007**, *79*, 2325−2338.
(4) (a) Ozment, C. P.; Turi, J. L. *Biochim. Biophys. Acta* **2009**, *1790*, 694−701. (b) Scott, L. E.; Orvig, C. *Chem. Rev.* **2009**, *109*, 4885−4910.
(5) Barbaro, M. P. F.; Carpagnano, G. E.; Spanevello, A.; Cagnazzo, M. G.; Barnes, P. J. *Int. J. Immunopathol. Pharmacol.* **2007**, *20*, 753−763.
(6) Raedschelders, K.; Ansley, D. M.; Chen, D. D. Y. *Pharmacol. Ther.* **2012**, *133*, 230−255.
(7) (a) Halliwell, B. *Biochem. J.* **2007**, *401*, 1−11. (b) Dizdaroglu, M.; Jaruga, P. *Free Radic. Res.* **2012**, *46*, 382−419.
(8) Brennan, L. A.; Kantorow, M. *Exp. Eye Res.* **2009**, *88*, 195−203.
(9) (a) Zang, L. Y.; Stone, K.; Pryor, W. A. *Free Radical Biol. Med.* **1995**, *19*, 161−167. (b) Guo, Q.; Zhao, B.; Shen, S.; Hou, J.; Hu, J.; Xin, W. *Biochim. Biophys. Acta* **1999**, *1427*, 13−23.
(10) (a) Zepp, R. G.; Faust, B. C.; Hoigne, J. *Environ. Sci. Technol.* **1992**, *26*, 313−319. (b) Vaughan, P. P.; Blough, N. V. *Environ. Sci. Technol.* **1998**, *32*, 2947−2953. (c) Takeda, K.; Takedoi, H.; Yamaji, S.; Ohta, K.; Sakugawa, H. *Anal. Sci.* **2004**, *20*, 153−158. (d) Linxiang, L.; Abe, Y.; Nagasawa, Y.; Kudo, R.; Usui, N.; Imai, K.; Mashino, T.; Mochizuki, M.; Miyata, N. *Biomed. Chromatogr.* **2004**, *18*, 470−474. (e) Liu, M.; Liu, S. M.; Peterson, S. L.; Miyake, M.; Liu, K. J. *Mol. Cell. Biochem.* **2002**, *234*, 379−385.
(11) (a) Soh, N.; Makihara, K.; Ariyoshi, T.; Seto, D.; Maki, T.; Nakajima, H.; Nakano, K.; Imato, T. *Anal. Sci.* **2008**, *24*, 293−296. (b) Newton, G. L.; Milligan, J. R. *Radiat. Phys. Chem.* **2006**, *75*, 473−478. (c) Saran, M.; Summer, K. H. *Free Radical Res.* **1999**, *31*, 429−436. (d) Qu, X. H.; Kirschenbaum, L. J.; Borish, E. T. *Photochem. Photobiol.* **2000**, *71*, 307−313. (e) Makrigiorgos, G. M.; Baranowska-Kortylewicz, J.; Bump, E.; Sahu, S. K.; Berman, R. M.; Kassis, A. I. *Int. J. Radiat. Biol.* **1993**, *63*, 445−458. (f) Soh, N.; Makihara, K.; Sakoda, E.; Imato, T. *Chem. Commun.* **2004**, 496−497.
(12) (a) Cui, G.; Ye, Z.; Chen, J.; Wang, G.; Yuan, J. *Talanta* **2011**, *84*, 971−976. (b) Koide, Y.; Kawaguchi, M.; Urano, Y.; Hanaoka, K.; Komatsu, T.; Abo, M.; Teraia, T.; Nagano, T. *Chem. Commun.* **2012**, *48*, 3091−3093. (c) Kundu, K.; Knight, S. F.; Willett, N.; Lee, S.; Taylor, W. R.; Murthy, N. *Angew. Chem., Int. Ed.* **2009**, *48*, 299−303.
(13) (a) Li, P.; Xie, T.; Duan, X.; Yu, F.; Wang, X.; Tang, B. *Chem.—Eur. J.* **2010**, *16*, 1834−1840. (b) Yapici, N. B.; Jockusch, S.; Moscatelli, A.; Mandalapu, S. R.; Itagaki, Y.; Bates, D. K.; Wiseman, S.; Gibson, K. M.; Turro, N. J.; Bi, L. R. *Org. Lett.* **2012**, *14*, 50−53. (c) Hong, J.; Zhuang, Y.; Ji, X.; Guo, X. *Analyst* **2011**, *136*, 2464−2470. (d) Pou, S.; Huang, Y. I.; Bhan, A.; Bhadti, V. S.; Hosmane, R. S.; Wu, S. Y.; Cao, G. L.; Rosen, G. M. *Anal. Biochem.* **1993**, *212*, 85−90. (e) Yang, X. F.; Guo, X. Q. *Analyst* **2001**, *126*, 1800−1804. (f) Yang, X. F.; Guo, X. Q. *Anal. Chim. Acta* **2001**, *434*, 169−177. (g) Maki, T.; Soh, N.; Fukaminato, T.; Nakajima, H.; Nakano, K.; Imato, T. *Anal. Chim. Acta* **2009**, *639*, 78−82.
(14) Page, S. E.; Wilke, K. T.; Pierre, V. C. *Chem. Commun.* **2010**, *46*, 2423−2425.
(15) (a) Thibon, A.; Pierre, V. C. *Anal. Bioanal. Chem.* **2009**, *394*, 107−120. (b) Bunzli, J. C. G.; Piguet, C. *Chem. Soc. Rev.* **2005**, *34*, 1048−1077.
(16) For recent representative examples see: (a) Lippert, A. R.; Gschneidtner, T.; Chang, C. J. *Chem. Commun.* **2010**, *46*, 7510−7512. (b) Kotova, O.; Comby, S.; Gunnlaugsson, T. *Chem. Commun.* **2011**, *47*, 6810−6812. (c) Weitz, E. A.; Chang, J. Y.; Rosenfield, A. H.; Pierre, V. C. *J. Am. Chem. Soc.* **2012**, *134*, 16099−16102. (d) Ye, Z. Q.; Chen, J. X.; Wang, G. L.; Yuan, J. L. *Anal. Chem.* **2011**, *83*, 4163−4169. (e) McMahon, B. K.; Gunnlaugsson, T. *J. Am. Chem. Soc.* **2012**, *134*, 10725−10728. (f) Pershagen, E.; Nordholm, J.; Borbas, K. E. *J. Am. Chem. Soc.* **2012**, *134*, 9832−9835. (g) Huang, K. W.; Marti, A. A. *Anal. Chem.* **2012**, *84*, 8075−8082. (h) Comby, S.; Tuck, S. A.; Truman, L. K.; Kotova, O.; Gunnlaugsson, T. *Inorg. Chem.* **2012**, *51*, 10158−10168. (i) Moore, J. D.; Lord, R. L.; Cisneros, G. A.; Allen, M. J. *J. Am. Chem. Soc.* **2012**, *134*, 17372−17375. (j) Thibon, A.; Pierre, V. C. *J. Am. Chem. Soc.* **2009**, *131*, 434−435.
(17) (a) Zhu, J.; Wang, X.-Z.; Chen, Y.-Q.; Jiang, X.-K.; Chen, X.-Z.; Li, Z.-T. *J. Org. Chem.* **2004**, *69*, 6221−6227. (b) Samuel, A. P. S.; Moore, E. G.; Melchior, M.; Xu, J.; Raymond, K. N. *Inorg. Chem.* **2008**, *47*, 7535−7544. (c) Adams, H.; Hunter, C. A.; Lawson, K. R.; Perkins, J.; Spey, S. E.; Urch, C. J.; Sanderson, J. M. *Chem.—Eur. J.* **2001**, *7*,

4863−4877. (d) Pecoraro, V. L.; Weit, F. L.; Raymond, K. N. *J. Am. Chem. Soc.* **1981**, *103*, 5133−5140.
(18) (a) Weitz, E. A.; Pierre, V. C. *Chem. Commun.* **2011**, *47*, 541−543. (b) Beeby, A.; M. Clarkson, I.; S. Dickins, R.; Faulkner, S.; Parker, D.; Royle, L.; de Sousa, A. S.; Gareth-Williams, J. A.; Woods, M. *J. Chem. Soc., Perkin Trans. 2* **1999**, 493−504. (c) Ghosh, P.; Federwisch, G.; Kogej, M.; Schalley, C. A.; Haase, D.; Saak, W.; Lutzen, A.; Gschwind, R. M. *Org. Biomol. Chem.* **2005**, *3*, 2691−2700. (d) Ay, E.; Chaumeil, H.; Barsella, A. *Tetrahedron* **2012**, *68*, 628−635.
(19) Horrocks, W. D.; Sudnick, D. R. *Acc. Chem. Res.* **1981**, *14*, 384−392.
(20) Winston, G. W.; Harvey, W.; Berl, L.; Cederbaum, A. I. *Biochem. J.* **1983**, *216*, 415−421.
(21) Gunnlaugsson, T.; Harte, A. J.; Leonard, J. P.; Nieuwenhuyzen, M. *Supramol. Chem.* **2003**, *15*, 505−519.
(22) Law, G.-L.; Pham, T. A.; Xu, J.; Raymond, K. N. *Angew. Chem., Int. Ed.* **2012**, *51*, 2371−2374.
(23) Gunnlaugsson, T.; Harte, A. J.; Leonard, J. P.; Nieuwenhuyzen, M. *Chem. Commun.* **2002**, 2134−2135.
(24) Herrmann, H.; Hoffmann, D.; Schaefer, T.; Braeuer, P.; Tilgner, A. *Chem. Phys. Chem.* **2010**, *11*, 3796−3822.
(25) Giorgio, M.; Trinei, M.; Migliaccio, E.; Pelicci, P. G. *Nat. Rev. Mol. Cell Biol.* **2007**, *8*, 722−728.
(26) Page, S. E.; Arnold, W. A.; McNeill, K. *J. Environ. Monitor.* **2010**, *12*, 1658−1665.